

# Quantum interferometry via a coherent state mixed with a photon-added squeezed vacuum state

Shuai Wang<sup>1,2†</sup>, Xuexiang Xu<sup>3</sup>, Yejun Xu<sup>4</sup>, Lijian Zhang<sup>2</sup>

<sup>1</sup> *School of Mathematics and Physics,  
Jiangsu University of Technology,  
Changzhou 213001, P.R. China*

<sup>†</sup> *Corresponding author: wshslxy@cczu.edu.cn*

<sup>2</sup> *College of Engineering and Applied Sciences, Nanjing University, Nanjing 210093, P.R. China*

<sup>3</sup> *Department of Physics, Jiangxi Normal University, Nanchang 330022, P.R. China and*

<sup>4</sup> *School of Mechanical and Electronic Engineering,  
Chizhou University, Chizhou 247000, P.R. China*

We theoretically investigate the phase sensitivity with parity detection on a Mach-Zehnder interferometer with a coherent state combined with a photon-added squeezed vacuum state. When the phase shift approaches zero, the squeezed vacuum state is indeed the optimal state within a constraint on the average number of photons. However, when the phase shift to be estimated slightly deviates from zero, the optimal state is neither the squeezed vacuum state nor the photon-subtracted squeezed vacuum state, but the photon-added squeezed vacuum state when they carry many photons. Finally, we show that the quantum Cramér-Rao bound can be reached by parity detection.

**PACS number(s):** 42.50.Dv, 03.65.Ta

## I. INTRODUCTION

Phase estimation and optimal interferometry play a significant role for many precision measurement applications. For a Mach-Zehnder interferometer (MZI), when only coherent light is injected into one input port of the first beam splitter, the other input port is by default the vacuum of light, the sensitivity of the phase estimation is limited by the standard quantum noise limit (SNL), i.e.,  $\Delta\phi \propto 1/\sqrt{\bar{N}}$ , where  $\bar{N}$  the average photon number in the input beam [1, 2]. When using a nonclassical input state, for example, a coherent light and a squeezed vacuum light are injected into the two input ports of a MZI, Caves [3] find that the sensitivity of phase estimation below the SNL. Since then, in order to go beyond the SNL, many highly nonclassical states are employed to reduce the phase uncertainty [3–15], and to approach  $\Delta\phi \propto 1/\bar{N}$ , the so-called Heisenberg limit (HL) [16, 17].

In general, the sensitivity of phase estimation within an interferometer crucially depends on input states as well as detection schemes. Coherent states and squeezed vacuum states as well as Fock states are useful for metrology under the present experimental technology. For example, via the analysis of the quantum Fisher information, for a MZI with a Fock state in one input port and an arbitrary state with the same total average photon number in the other input, same phase uncertainties will be achieved and can approach to the HL [18]. Following the theoretical work in Ref. [18], we analytically prove that the quantum Cramer-Rao bound can be reached via the parity detection in the limit  $\varphi \rightarrow 0$  [19]. By Bayesian analysis of the photon number statistics of the output state in a MZI, Pezzé and Smerzi show that the HL sensitivity of phase estimation can be achieved when the coherent light and squeezed vacuum light are mixed in roughly equal

intensities [20]. As a simple alternative to the detection scheme of Ref.[20], parity detection for a MZI with coherent and squeezed vacuum light has been also investigated [21]. A parity measurement simply measures the even or odd number of photons in the output mode [22].

Recently, Lang and Caves have considered the question: given that one input of an interferometer is entered by coherent light, what is the best state to inject the other input port for achieving high-sensitivity phase-shift measurements within a constraint on the average photon number that the state can carry? The answer, they find, is the squeezed vacuum state (SVS) [23]. As just pointed out in the conclusion in Ref. [23], it needs to further investigate whether the SVS is the optimal state when the squeezing light carries many photons, even carries as many or more photons than the coherent input. On the other hand, when the phase shift to be estimated slightly deviates from zero, whether the SVS with many photons is also the optimal state? For fixed initial squeezing parameter, Birrittella and Gerry claim that the corresponding sensitivity of the phase estimation can be increased via parity detection when the mixing of coherent states and photon-subtracted SVS (PSSVS) as input states of the MZI [24]. However, within a constraint on the total average photon number, whether the PSSVS can indeed improve the phase sensitivity?

In this work, we will answer the above questions by investigating the interferometry performed by mixing a coherent state with non-Gaussian squeezed states, such as a photon-added SVS (PASVS) and the PSSVS. At present, the best experimentally realized non-Gaussian squeezed state in quantum optics is the photon-subtracted squeezed states [25, 26], and photon subtraction can be implemented by a beam splitter with high transmissivity [25]. For the photon addition operation,

Agarwal and Tara [26] first theoretically studied the non-classical properties of a photon-added coherent state. In 2004, the photon addition operation was successfully demonstrated experimentally via a non-degenerate parametric amplifier with small coupling strength [28]. We also compared the phase sensitivity with another quantum limit, the quantum Cramér-Rao bound [29], which sets the ultimate limit for a set of probabilities that originated from measurements on a quantum system.

The organization of this paper is as follows. In Sec. II, we make a brief review about both the PASVS and the PSSVS. And then we describes the propagation of a two-mode light, initially in the product state of PASVS and coherent light, through the MZI. Section III focuses on the parity detection scheme and provides the phase sensitivity. We will show that for giving a constraint on the average photon numbers of PASVS/PSSVS/SVS, almost the same phase sensitivity will be achieved by parity detection with such kinds of input states. Especially, when the phase shift slightly deviates from zero, the optimal state is neither the SVS nor the PSSVS, but the PASVS when they carry many photons. In Sec. IV, we prove that the quantum Cramer-Rao bound can be reached via the parity detection in the limit  $\varphi \rightarrow 0$ .

## II. RESULTED OUTPUT STATE OF THE INPUT FIELDS THROUGH THE INTERFEROMETER

Previously, Birrittella and Gerry [24] studied the prospect of parity-based interferometry with mixing a PSSVS and a coherent state. In contrast to that scheme, we mainly investigate the scheme when a PASVS and a coherent state ( $|z\rangle$  with the amplitude parameter  $z = |z|e^\theta$ ) are considered as the input state of a MZI. For our purposes, we first provide a brief review of both the PASVS and the PSSVS which is a kind of non-Gaussian squeezed vacuum states. And then, we derive the resulted output state when a PASVS and a coherent state are injected into a balanced MZI

### A. Photon-added and photon-subtracted squeezed vacuum states

The SVS is a Gaussian state, which is defined as [30]

$$|r\rangle = S(r)|0\rangle = \text{sech}^{1/2}r \exp\left(-\frac{1}{2}b^{\dagger 2} \tanh r\right)|0\rangle, \quad (1)$$

where  $S(r) = \exp[r(b^2 - b^{\dagger 2})/2]$  with the squeezing parameter  $r$ . By repeatedly operating the photon addition operator  $b^\dagger$  on a SVS, one obtain the normalized PASVS which is defined as

$$|r, k\rangle = \frac{1}{\sqrt{N_k}} b^{\dagger k} S(r)|0\rangle, \quad (2)$$

where  $N_k$  is the corresponding normalization factor [31]

$$\begin{aligned} N_k &= \frac{\partial^{2k}}{\partial t^k \partial \tau^k} \exp\left[-\frac{\sinh 2r}{4}(t^2 + \tau^2) + t\tau \cosh^2 r\right] \Big|_{t, \tau=0} \\ &= k! \cosh^k r P_k(\cosh r). \end{aligned} \quad (3)$$

The average photon number of the PASVS is given by

$$\bar{n}_a = \langle b^\dagger b \rangle_{\text{PASVS}} = \frac{N_{k+1}}{N_k} - 1. \quad (4)$$

Different from that in Ref.[24], we adopt the expression of the PSSVS as following

$$|r, -l\rangle = \frac{1}{\sqrt{C_l}} b^l S(r)|0\rangle, \quad (5)$$

where  $b$  is the photon subtraction operator, and the normalization factor is [32]

$$\begin{aligned} C_l &= \frac{\partial^{2l}}{\partial t^l \partial \tau^l} \exp\left[-\frac{\sinh 2r}{4}(t^2 + \tau^2) + t\tau \sinh^2 r\right] \Big|_{t, \tau=0} \\ &= l! (-i \sinh r)^l P_l(i \sinh r). \end{aligned} \quad (6)$$

The average photon number of the PSSVS is given by

$$\bar{n}_s = \langle b^\dagger b \rangle_{\text{PSSVS}} = \frac{C_{k+1}}{C_k}. \quad (7)$$

Particularly, when  $k = l$ , the single-photon PASVS and the single-photon PSSVS are the same non-Gaussian squeezed state [33].

For the quantum metrology, the average photon number of input states is an important factor. Actually, both photon addition and subtraction can increase the average photon number of the state as shown in Fig. 1. Clearly, it is always better to perform addition rather than subtraction in order to increase the average photon number for given the initial squeezing. And hence, we expect that the PASVS can offer an improved phase resolution over both the PSSVS-coherent input state and SVS-coherent input state for a given initial squeezing parameter of the SVS. The fact that the photon subtraction can increase the average photon number of the states with super-Poissonian statistics was explained in detail very recently by Stephen et al [34] and references involved in that. Indeed, the distribution for the single-mode SVS, as is well known, is super-Poissonian [35].

### B. Resulted output state of the PASVS through the interferometer

The balanced MZI considered here is mainly composed of two 50:50 beam splitters and two phase shifters. Generally, the first beam splitter BS1 is described by the transformation  $U_{\text{BS1}} = \exp[-i\pi(a^\dagger b + ab^\dagger)/4]$ . And the operator representation of the second beam splitter BS2 is taken as  $U_{\text{BS2}} = \exp[i\pi(a^\dagger b + ab^\dagger)/4]$ . The operator  $U(\varphi) = \exp[i\varphi(a^\dagger a - b^\dagger b)/2]$  represents the two phase

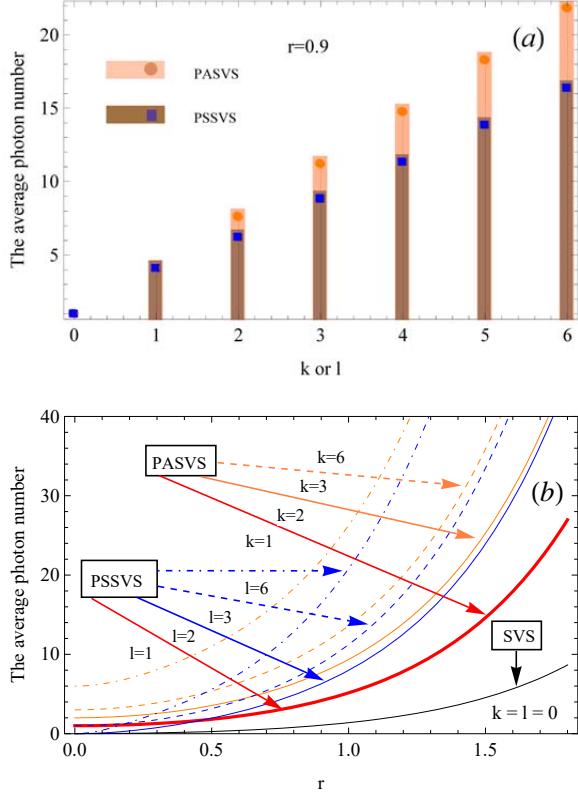


FIG. 1. Plots of the average photon number of both the PASVS and the PSSVS, as well as the SVS, respectively. (a) The average photon number for a given SVS (fixed squeezing parameter  $r$ ) as a function of the number  $k$  or  $l$ ; (b) The average photon number as a function of the squeezing parameter  $r$  for some values of  $k$  and  $l$ .

shifters, the angle  $\varphi$  being the phase shift between the two arms to be estimated. The unitary transformation associated with such balanced MZI can be written as [14]

$$U(\varphi) = e^{i\frac{\pi}{2}J_1} e^{-i\varphi J_3} e^{-i\frac{\pi}{2}J_1} = e^{-i\varphi J_2}, \quad (8)$$

where these operators consisted of two sets of Bose operator

$$\begin{aligned} J_1 &= \frac{1}{2}(a^\dagger b + ab^\dagger), \quad J_2 = \frac{1}{2i}(a^\dagger b - ab^\dagger), \\ J_3 &= \frac{1}{2}(a^\dagger a - b^\dagger b), \end{aligned} \quad (9)$$

are the angular momentum operators in the well-known Schwinger representation [36]. They satisfy the commutation relation  $[J_i, J_j] = i\epsilon_{ijk}J_k$  ( $i, j, k = 1, 2, 3$ ), and commute with the Casimir operator  $J_0 = \frac{1}{2}(a^\dagger a + b^\dagger b)$ , i.e.,  $[J_0, J_i] = 0$ . Propagation of the input fields (pure states) through these elements, the resulted output state can be written as

$$|\text{out}\rangle_{\text{MZI}} = e^{-i\varphi J_2} |\psi\rangle_{\text{in}}. \quad (10)$$

For the balanced MZI, applying the following transformation relations

$$\begin{aligned} e^{-i\varphi J_2} a^\dagger e^{i\varphi J_2} &= a^\dagger \cos \frac{\varphi}{2} + b^\dagger \sin \frac{\varphi}{2}, \\ e^{-i\varphi J_2} b^\dagger e^{i\varphi J_2} &= b^\dagger \cos \frac{\varphi}{2} - a^\dagger \sin \frac{\varphi}{2} \end{aligned} \quad (11)$$

and the relation  $e^{-i\varphi J_2} |0\rangle_a |0\rangle_b = |0\rangle_a |0\rangle_b$ , in principle, one can obtain the explicit form of the output state the MZI.

For the convenience of the later calculation, we rewrite the PASVS  $|\psi_{r,k}\rangle_b$  in the basis of the coherent state as follows

$$|\psi_{r,k}\rangle_b = \frac{\text{sech}^{1/2} r}{\sqrt{N_k}} \frac{d^k}{dg^k} \int \frac{d^2\alpha}{\pi} e^{-\frac{|\alpha|^2}{2} + g\alpha^* - \frac{\tanh r}{2} \alpha^{*2}} |\alpha\rangle |g=0\rangle, \quad (12)$$

where  $|\alpha\rangle = \exp[-|\alpha|^2/2 + \alpha b^\dagger] |0\rangle$  is a coherent state. When the product state  $|\psi\rangle_{\text{in}} = |z\rangle_a \otimes |\psi_{r,k}\rangle_b$  is injected into the MZI, the resulted output state can be written as

$$|\psi\rangle_{\text{out}} = \frac{\text{sech}^{1/2} r}{\sqrt{N_k}} \frac{d^k}{dg^k} \int \frac{d^2\alpha}{\pi} e^{-\frac{|z|^2}{2} - |\alpha|^2 + g\alpha^* - \frac{\tanh r}{2} \alpha^{*2}} e^{(\alpha \sin \frac{\varphi}{2} + z \cos \frac{\varphi}{2}) a^\dagger + (\alpha \cos \frac{\varphi}{2} - z \sin \frac{\varphi}{2}) b^\dagger} |0, 0\rangle |g=0\rangle, \quad (13)$$

which is the state of light at the output of the MZI. In the following section, we shall mainly present parity measurement scheme with calculations of the expected value of the parity operator and the corresponding phase sensitivity.

### III. PHASE ESTIMATION WITH PARITY DETECTION

There are several detection methods for extracting phase information from the output states of the MZI, e.g., intensity detection, homodyne detection, and parity detection [22]. Parity detection simply measures the even or odd number of photons in the output mode. In addition, as shown in Ref. [21], the parity detection saturates the quantum Cramér-Rao bound and in turn provides the HL phase sensitivity when the SVS-coherent state are mixed in equal proportions. In experiments, the parity detection using a photon-number resolving detector with coherent states [37] has also been demonstrated. Here, we use the parity detection too.

#### A. The parity detection with the PASVS-coherent state

For the detailed discussion of the parity detection in quantum optimal metrology, one can review that in Ref.[22]. Actually, the parity detection is to obtain the expectation value of the parity operator in the output state of the MZI. In order to calculate conveniently, using the operator identity

$\exp(\lambda a^\dagger a) =: \exp[(e^\lambda - 1) a^\dagger a] :$ , we rewrite the parity operator as follows

$$\Pi_b = (-1)^{b^\dagger b} = e^{i\pi b^\dagger b} =: e^{-2b^\dagger b} : = \int \frac{d^2\gamma}{\pi} |\gamma\rangle \langle -\gamma|, \quad (14)$$

where  $|\gamma\rangle$  is a coherent state, and  $: :$  denotes the normally ordered form of Bose operators. Here, we consider performing parity detection on just one of the output modes, for instance, the  $b$  mode. The parity operator on an output mode  $b$  is described by  $\Pi_B = (-1)^{b^\dagger b}$ , then the expectation value of the parity operator is

$$\langle \Pi_b(\varphi) \rangle =_{\text{out}} \langle \psi | \int \frac{d^2\gamma}{\pi} |\gamma\rangle \langle -\gamma | | \psi \rangle_{\text{out}}. \quad (15)$$

Now, we consider the corresponding the expectation value of the parity operator in the output state when the PASVS-coherent state is injected into the MZI. Then substituting Eqs. (13) and (14) into Eq. (15), and applying the integral formula

$$\int \frac{d^2z}{\pi} e^{\zeta|z|^2 + \xi z + \eta z^* + f z^2 + g z^{*2}} = \frac{1}{\sqrt{\zeta^2 - 4fg}} e^{\frac{-\zeta\xi\eta + \xi^2g + \eta^2f}{\zeta^2 - 4fg}} \quad (16)$$

whose convergent condition is  $\text{Re}(\xi \pm f \pm g) < 0$  and  $\text{Re}\left(\frac{\zeta^2 - 4fg}{\xi \pm f \pm g}\right) < 0$ , after directly calculation, we obtain

$$\begin{aligned} \langle \Pi_b(\varphi) \rangle_{\text{PA}} &= \frac{\langle \Pi_b(\varphi) \rangle_0}{N_k} \frac{\partial^{2k}}{\partial h^k \partial g^k} \exp \left[ -\frac{\cosh^2 r \cos \varphi}{1 + \sin^2 \varphi \sinh^2 r} gh \right. \\ &\quad + \frac{4z \cosh^2 r \sin \varphi + z^* \sinh 2r \sin 2\varphi}{4(1 + \sin^2 \varphi \sinh^2 r)} h \\ &\quad + \frac{4z^* \cosh^2 r \sin \varphi + z \sinh 2r \sin 2\varphi}{4(1 + \sin^2 \varphi \sinh^2 r)} g \\ &\quad \left. - \frac{\sinh 2r \cos^2 \varphi}{4(1 + \sinh^2 r \sin^2 \varphi)} (h^2 + g^2) \right] \Big|_{h=g=0}, \quad (17) \end{aligned}$$

where  $\langle \Pi_b \rangle_0$  is the corresponding expectation value of the parity operator for the input state with SVS-coherent state [21],

$$\langle \Pi_b(\varphi) \rangle_0 = \frac{e^{\frac{2(\cos \varphi - 1 - \sinh^2 r \sin^2 \varphi)|z|^2 - \sinh 2r \sin^2 \varphi \text{Re}(z^2)}{2(1 + \sinh^2 r \sin^2 \varphi)}}}{\sqrt{1 + \sinh^2 r \sin^2 \varphi}}. \quad (18)$$

Because the goal of the interferometry is to estimate very small phase changes in quantum metrology, it may be interesting to expand Eq. (17) in the Taylor series around  $\varphi = 0$ . To write out the explicit Taylor expansion of Eq. (17) for general  $k$  in the limit  $\varphi \rightarrow 0$  is a difficult task. However, for small  $k$ , the explicit Taylor expansions can be accessible. When  $k = 0$ , the Taylor expansions of  $\langle \Pi_b(\varphi) \rangle_0$  is

$$\begin{aligned} &\langle \Pi_b(\varphi \rightarrow 0) \rangle_0 \\ &= \left[ 1 - \bar{n}_z \cos \theta \sqrt{\bar{n}_a^2 + \bar{n}_a + 1} \varphi^2 \right. \\ &\quad \left. - \frac{2\bar{n}_z \bar{n}_a + \bar{n}_z + \bar{n}_a}{2} \varphi^2 + O(\varphi^4) \right], \quad (19) \end{aligned}$$

where  $\bar{n}_z = |z|^2$  ( $z = |z|e^{i\theta}$ ) the average photon number of the coherent state,  $\bar{n}_a = (N_{k+1}/N_k - 1)|_{k=0} = \sinh^2 r$  the average photon number of the SVS. While  $k = 1, 2$ , we can derive the analytical Taylor expansions of  $\langle \Pi_b(\varphi) \rangle_{\text{PA}}$  as well, i.e.,

$$\begin{aligned} &\langle \Pi_b(\varphi \rightarrow 0) \rangle_{\text{PA}} |_{k=1} \\ &= (-1) \left[ 1 - \bar{n}_z \cos \theta \sqrt{\bar{n}_a^2 + \bar{n}_a - 2} \varphi^2 \right. \\ &\quad \left. - \frac{2\bar{n}_z \bar{n}_a + \bar{n}_z + \bar{n}_a}{2} \varphi^2 + O(\varphi^4) \right], \quad (20) \end{aligned}$$

and

$$\begin{aligned} &\langle \Pi_b(\varphi \rightarrow 0) \rangle_{\text{PA}} |_{k=2} \\ &= \left[ 1 - \bar{n}_z \cos \theta \sqrt{\bar{n}_a^2 + \bar{n}_a - \frac{8(\sqrt{1+12\bar{n}_a}+1)^2}{3(\sqrt{1+12\bar{n}_a}-1)^2}} \varphi^2 \right. \\ &\quad \left. - \frac{2\bar{n}_z \bar{n}_a + \bar{n}_z + \bar{n}_a}{2} \varphi^2 + O(\varphi^4) \right], \quad (21) \end{aligned}$$

where  $\bar{n}_a = N_{k+1}/N_k - 1$  the average photon number of the PASVS. In order to obtain the good phase uncertainty, in the following we set  $\theta = 0$  (the phase of the coherent state) [21]. These analytical Taylor expansions of  $\langle \Pi_b(\varphi) \rangle_{\text{PA}}$  mentioned above is useful for the following discussions about the parity detection.

Different from that calculation method in Ref.[24], for the normalized PSSVS, using our method, we can also obtain the corresponding expectation value of the parity operator for the input state with PSSVS-coherent states

$$\begin{aligned} \langle \Pi_b(\varphi) \rangle_{\text{PS}} &= \frac{\langle \Pi_b(\varphi) \rangle_0}{C_l} \frac{\partial^{2l}}{\partial h^l \partial g^l} \exp \left[ -\frac{\sinh^2 r \cos \varphi}{1 + \sin^2 \varphi \sinh^2 r} gh \right. \\ &\quad - \frac{z \sinh^2 r \sin 2\varphi + z^* \sinh 2r \sin \varphi}{2(1 + \sin^2 \varphi \sinh^2 r)} g \\ &\quad - \frac{z^* \sinh^2 r \sin 2\varphi + z \sinh 2r \sin \varphi}{2(1 + \sin^2 \varphi \sinh^2 r)} h \\ &\quad \left. - \frac{\sinh r \cosh r}{2(1 + \sin^2 \varphi \sinh^2 r)} (h^2 + g^2) \right] \Big|_{h=g=0}, \quad (22) \end{aligned}$$

Although Eq. (22) is different from Eq. (16) in Ref.[24], one can prove that two results are completely identical by numerical method. In addition, when  $k = l = 1$ , one can obtain  $\langle \Pi_b(\varphi) \rangle_{\text{PS}} |_{l=1} = \langle \Pi_b(\varphi) \rangle_{\text{PA}} |_{k=1}$ , this is because

one photon-subtracted SVS is identical to one photon-added SVS [33]. When  $l = 2$ , the Taylor expansion of  $\langle \Pi_b(\varphi) \rangle_{\text{PS}}$  in the limit  $\varphi \rightarrow 0$  is

$$\langle \Pi_b(\varphi) \rangle_{\text{PS}} |_{l=2} = \left[ 1 - \bar{n}_z \cos \theta \sqrt{\bar{n}_s^2 + \bar{n}_s - \frac{8(\sqrt{1+12\bar{n}_s}-1)^2}{3(\sqrt{1+12\bar{n}_s}+1)^2} \varphi^2} - \frac{2\bar{n}_z\bar{n}_s + \bar{n}_z + \bar{n}_s}{2} \varphi^2 + O(\varphi^4) \right] \quad (23)$$

where  $\bar{n}_s = C_{l+1}/C_l$  the average photon number of the PSSVS.

By Eqs. (17) and (22), we can investigate the expectation value of the parity operator as function of the phase shift  $\varphi$ . Given  $r = 0.3$  and  $z = 2$ , in Fig. 2(a) we draft this expectation value against  $\varphi$  for  $k = 0, 1, 2, 3$  and  $l = 0, 1, 2, 3$ . One can see that, for the central peak or trough of the  $\langle \Pi_b(\varphi) \rangle$ , the narrowness of the maxima or minima at  $\varphi = 0$  increases as  $k$  and  $l$  increase. In addition, we see that the central peak or trough of the  $\langle \Pi_b \rangle_{\text{PA}}$  of the PASVS-coherent input states is narrower than that of the PSSVS-coherent input states when  $k = l > 1$ . This result indicates that the photon addition can enhance super-resolution better than photon subtraction for given initial coherent state amplitude and squeezing parameters. However, if given the same average photon number ( $\bar{n}_a = \bar{n}_s$ ) of both the PASVS and the PSSVS, the distributions of these central peaks or troughs of the  $\langle \Pi_b(\varphi) \rangle$  near  $\varphi = 0$  are almost identical as shown in Fig. 2(b), which is also consistent with Eqs. (19-21) and (23).

### B. Phase sensitivity via the error propagation method

The phase uncertainty  $\Delta\varphi$  is the main aspect of quantum optimal interferometry. The smallest phase uncertainty  $\Delta\varphi$  is the characteristic of the most sensitive measure. The smaller the value of  $\Delta\Pi_b$  is, the higher the phase sensitivity is. From the error propagation method, the phase uncertainty  $\Delta\varphi$  of an interferometer can be determined as

$$\Delta\varphi = \frac{\sqrt{1 - \langle \Pi_b(\varphi) \rangle^2}}{|\partial \langle \Pi_b(\varphi) \rangle / \partial \varphi|} \quad (24)$$

where we have used  $\Delta\Pi_b = \sqrt{\langle \Pi_b^2(\varphi) \rangle - \langle \Pi_b(\varphi) \rangle^2}$  and the fact that  $\langle \Pi_b^2(\varphi) \rangle = 1$ . The phase sensitivity with parity detection for the interferometry with PASVS-coherent state is found to be best at  $\varphi = 0$ . Although it is difficult to write out the general explicit form of Eq. (24) when the PASVS-coherent state with the general value of  $k$  is considered as an interferometer state, based on Eqs. (19-21), the explicitly forms of  $\Delta\varphi$  for small  $k$  in the limit of  $\varphi \rightarrow 0$  can be easily obtained. For example,

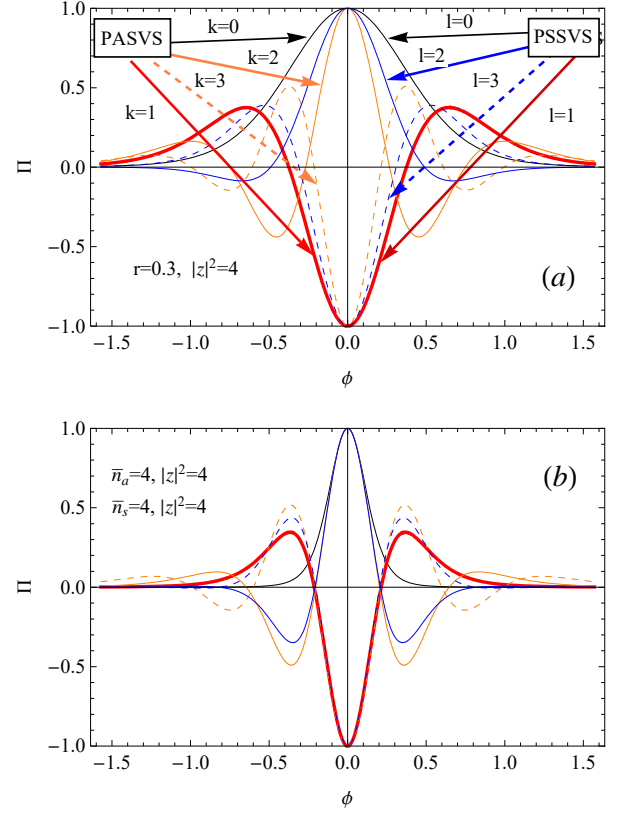


FIG. 2. The expectation value of the parity operator versus the phase shift  $\varphi$  for different PASVS-coherent and PSSVS-coherent input states of the MZI, respectively.

according to Eq. (19), the explicit form of Eq. (24) in the case of  $\varphi \rightarrow 0$  can be directly obtained [21],

$$(\Delta\varphi)_{\text{PA}} |_{k=0} = \frac{1}{\sqrt{2\bar{n}_z \sqrt{\bar{n}_a^2 + \bar{n}_a + 1} + 2\bar{n}_z\bar{n}_a + \bar{n}_z + \bar{n}_a}}, \quad (25)$$

where they have set  $\theta = 0$  (the phase of the coherent state) in order to obtain the good phase uncertainty. In addition, based on our Eqs. (20) and (21), we can also obtain the explicit form of Eq. (24) for  $k = 1, 2$ , respectively,

$$(\Delta\varphi)_{\text{PA}} |_{k=1} = \frac{1}{\sqrt{2\bar{n}_z \sqrt{\bar{n}_a^2 + \bar{n}_a - 2} + 2\bar{n}_z\bar{n}_a + \bar{n}_z + \bar{n}_a}}, \quad (26)$$

and

$$(\Delta\varphi)_{\text{PA}} |_{k=2} = \frac{1}{\sqrt{2\bar{n}_z \sqrt{\bar{n}_a^2 + \bar{n}_a - \frac{8(\sqrt{1+12\bar{n}_a}+1)^2}{3(\sqrt{1+12\bar{n}_a}-1)^2}} + 2\bar{n}_z\bar{n}_a + \bar{n}_z + \bar{n}_a}} \quad (27)$$

For the item  $\frac{8(\sqrt{1+12\bar{n}_a+1})^2}{3(\sqrt{1+12\bar{n}_a-1})}$  in Eq. (27), one can easily obtain  $\frac{8(\sqrt{1+12\bar{n}_a+1})^2}{3(\sqrt{1+12\bar{n}_a-1})}|_{k=2} = \frac{24 \cosh^4 r}{(3 \cosh^2 r - 1)^2}$ , and prove that the inequality  $\frac{8}{3} \leq \frac{8(\sqrt{1+12\bar{n}_a+1})^2}{3(\sqrt{1+12\bar{n}_a-1})} \leq 6$  for any values of the squeezing parameter  $r$  is satisfied. On the other hand, when the PSSVS-coherent state with  $l = 2$  is considered as the interferometer state, according to Eq. (23), we obtain the corresponding phase uncertainty in the case of  $\varphi \rightarrow 0$  as

$$(\Delta\varphi)_{\text{PS}}|_{l=2} = \frac{1}{\sqrt{2\bar{n}_z} \sqrt{\bar{n}_s^2 + \bar{n}_s - \frac{8(\sqrt{1+12\bar{n}_s-1})^2}{3(\sqrt{1+12\bar{n}_s+1})} + 2\bar{n}_z\bar{n}_s + \bar{n}_z + \bar{n}_s}} \quad (28)$$

where we have set  $\theta = 0$  as well. For the item  $\frac{8(\sqrt{1+12\bar{n}_s-1})^2}{3(\sqrt{1+12\bar{n}_s+1})}|_{l=2} = \frac{24 \sinh^4 r}{(3 \sinh^2 r + 1)^2}$  in Eq. (28), one can easily prove that the inequality  $0 \leq 24 \sinh^4 r / (3 \sinh^2 r + 1)^2 \leq \frac{8}{3}$  is satisfied.

Obviously, Eqs. (25-28) indicate that, within constraints on the total average photon number ( $\bar{N} = \bar{n}_a + \bar{n}_z$  or  $\bar{N} = \bar{n}_s + \bar{n}_z$ ) and the same ratios of  $\bar{n}_a/\bar{n}_z$  or  $\bar{n}_s/\bar{n}_z$ , the best phase uncertainty is obtained by the SVS when one input port of a MZI is injected by a coherent state. When  $k = l = 0$ , both PASVS and PSSVS reduce to a SVS. Therefore, our results obtained via parity detection indeed support Lang and Caves's work that the SVS is the optimal state for a MZI in the limit of  $\varphi \rightarrow 0$  when one input is a coherent state [23]. On the other hand, given a larger value of the same average photon numbers of the PASVS, the PSSVS and the SVS, we can also see from Eqs. (25-28) that the difference among these corresponding phase uncertainties is very small. With the increases of the values of the  $k$  and  $l$ , we can numerically prove such conclusion is still true. As pointed in Refs. [20, 23], we can also prove that, in the case of the  $\bar{n}_a = \bar{n}_z$  (or  $\bar{n}_s = \bar{n}_z$ ), the best phase sensitivity will be obtained and reach the HL.

However, when the phase shift  $\varphi$  to be estimated slightly deviates from zero, the SVS with many photons may be not the optimal state for a MZI. Firstly, we investigate how the phase uncertainty varies with  $\varphi$ . Based on Eq. (24), we plot the phase uncertainty as a function of the phase shift  $\varphi$  in Fig. 3. Fig. 3(a) shows that, given somewhat small average photon numbers  $\bar{n}_a = \bar{n}_s = \bar{n}_z = 4$ , the MZI with one input port injected by a coherent state, the SVS state is the optimal state for such MZI. Yet, interferometry with coherent states contained a few average number of photons is meaningless since such a measurement cannot be precise in principle. Moreover as pointed in the conclusion part in Ref. [23], it may interesting to explore how the phase sensitivity changes when the SVS carry many photons. Thus, with the increases of the value of  $\bar{n}_a$  (or  $\bar{n}_s$ ) and  $\bar{n}_z$ , we can see from Fig. 3(b) that the differences among

these corresponding phase uncertainties are indeed very small in the limit of  $\varphi \rightarrow 0$ . While the phase shift  $\varphi$  deviates from zero, the optimal state is neither the SVS nor the PSSVS, but the PASVS as shown in Fig. 3(b). On the other hand, for a given initial squeezing parameter  $r$  or given the same ratio of  $\bar{n}_a/\bar{n}_z$  (and  $\bar{n}_s/\bar{n}_z$ ) of the two input ports of the MZI, the PASVS has also the better performance in quantum precision measurement than both the PSSVS and the SVS when the phase shift  $\varphi$  slightly deviates from zero as shown in Fig. 4.

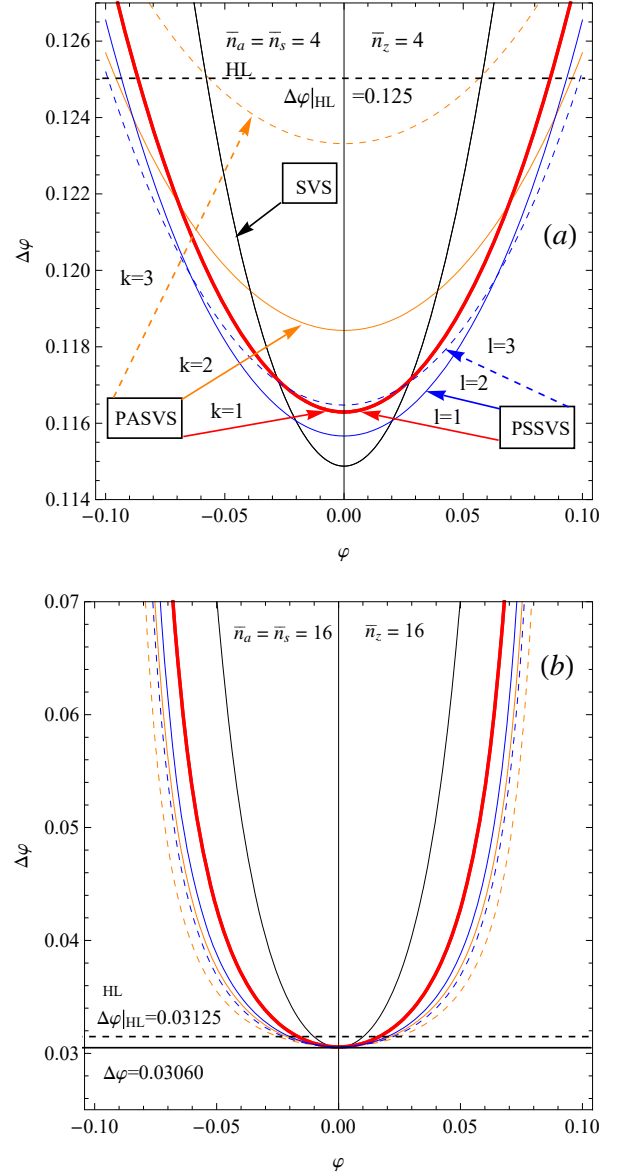


FIG. 3. The phase uncertainty  $\Delta\varphi$  as a function of the phase shift  $\varphi$  when the PASVS-coherent state, the PSSVS-coherent state and the SVS-coherent state as interferometer states, respectively. (a)  $\bar{n}_a = \bar{n}_s = \bar{n}_z = 4$ ; (b)  $\bar{n}_a = \bar{n}_s = \bar{n}_z = 16$ . The horizontal dashed line denotes the HL limit.

Secondly, for given a constraint on the total average photon number of the PASVS, the PSSVS and the SVS,

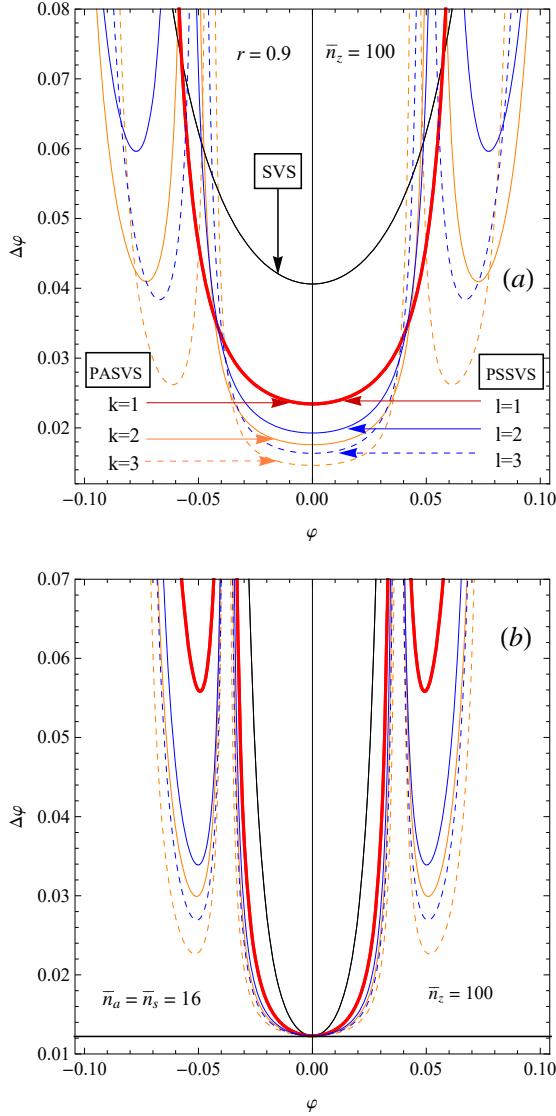


FIG. 4. The phase uncertainty  $\Delta\varphi$  as a function of the phase shift  $\varphi$  when the PASVS-coherent state, the PSSVS-coherent state and the SVS-coherent state as interferometer states. (a)  $r = 0.9, \bar{n}_z = 100$ ; (b)  $\bar{n}_a = \bar{n}_s = 16, \bar{n}_z = 100$ .

it is important to investigate how the phase sensitivities change with the total average photon number. In Fig. 5, for the PASVS ( $k = 0, 1, 2, 3, 6$ ) and the PSSVS ( $l = 0, 1, 2, 3, 6$ ), we give some same values of both  $\bar{n}_a$  and  $\bar{n}_s$  and plot the phase sensitivities versus the total number of photons  $\bar{N}$ . Obviously, from Fig. 5 we can see that almost the same phase uncertainties can be obtained in the limit of  $\varphi \rightarrow 0$ . In addition, when the values of both  $\bar{n}_a$  and  $\bar{n}_s$  increase, these phase uncertainties more quickly approach to the HL. Of course, when  $\bar{n}_a = \bar{n}_z$  (or  $\bar{n}_s = \bar{n}_z$ ), the optimal phase uncertainties will be obtained. In Fig. 6, we repeat these graphs for  $\varphi = 0.015$ . In the latter case especially, we see that the optimal state is the PASVS. When  $\bar{n}_a$  and  $\bar{n}_s$  increase, the phase uncertainties blow up due to the periodic na-

ture of the expectation value of the parity operator, but there are other photon numbers where the uncertainty is still below the SNL for both the PASVS and the PSSVS.

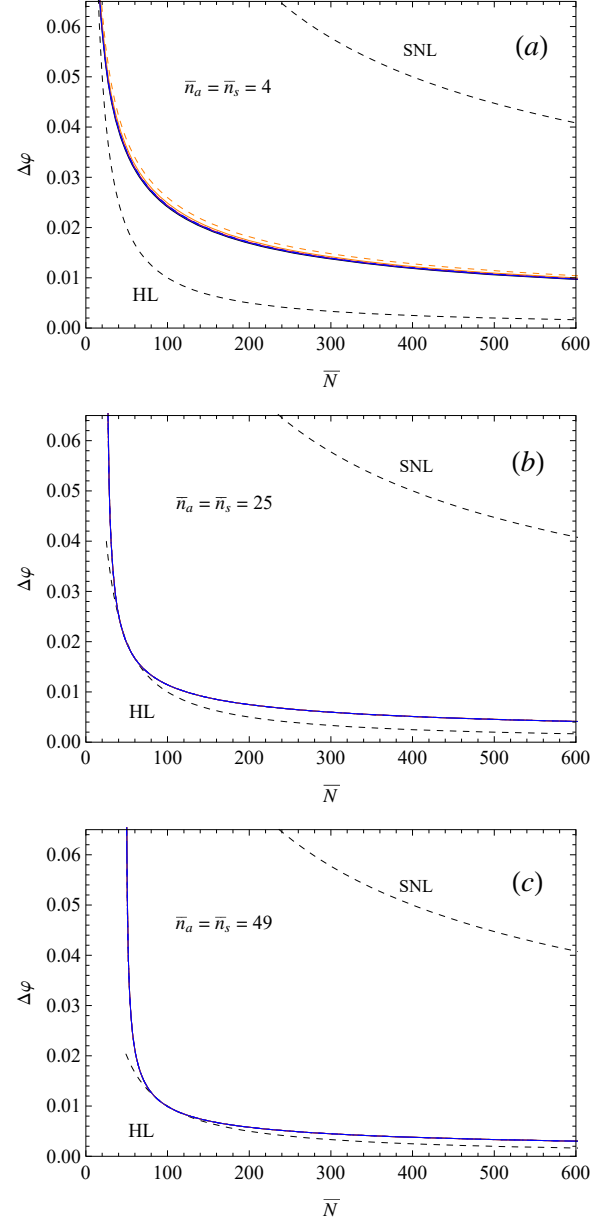


FIG. 5. Plots of the phase uncertainty versus total average photon at  $\varphi = 10^{-4}$  for fixed the average photon number of the PASVS and the PSSVS, as well as the SVS, along with the corresponding curves for the SNL and the HL limits. Only the parameter  $\bar{n}$  is being changed.

Finally, we further investigate how the photon addition and subtraction affect the phase sensitivity for a given initial squeezing parameter of the SVS. Comparing with that results in Ref. [24], we find that, for the same initial squeezing parameter  $r$ , it is also better to perform photon addition rather than photon subtraction

in respect to reducing the phase uncertainty. This is because that it is always better to perform photon addition rather than photon subtraction in order to increase the average photon number for given the initial squeezing as shown in Fig. 1.

#### IV. QUANTUM FISHER INFORMATION OF THE MZI INTERFEROMETER

In this section, we will prove that the parity detection is the optimal measurement for our considered interferometric scheme. Now, we use the quantum Fisher information to find the maximum level of the phase sensitivity by the Cramér–Rao bound as given by [17]

$$\Delta\varphi_{\min} = \frac{1}{\sqrt{F_Q}}, \quad (29)$$

For pure states injected into a MZI, the quantum Fisher information  $F_Q$  can be obtained by [38]

$$F_Q = 4 \left[ \langle \psi'(\varphi) | \psi'(\varphi) \rangle - |\langle \psi'(\varphi) | \psi(\varphi) \rangle|^2 \right], \quad (30)$$

where  $|\psi(\varphi)\rangle = e^{-i\varphi J_3} e^{-i\pi J_1/2} |\psi\rangle_{\text{in}}$  is the state just before the second beam splitter of the MZI, and  $|\psi'(\varphi)\rangle = \partial|\psi(\varphi)\rangle/\partial\varphi$ . In terms of the input state, the quantum Fisher information becomes

$$F_Q = 4 \left[ \langle \text{in} | J_2^2 | \text{in} \rangle - |\langle \text{in} | J_2 | \text{in} \rangle|^2 \right], \quad (31)$$

and thus the quantum Fisher information is, up to factor of 4, the variance of the operator  $J_2$ .

In the present work, the PASVS-coherent state as the interferometer state. In order to obtain the quantum Fisher information, based on Eqs. (2) and (3), we first obtain the following expectation values, i.e.,  $\langle b \rangle_{\text{PASVS}} = \langle b^\dagger \rangle_{\text{PASVS}} = 0$ , and

$$\begin{aligned} N_{k+2,k} &\equiv \langle b^2 \rangle_{\text{PASVS}} \\ &= \frac{\partial^{2k+2}}{\partial t^{k+2} \partial \tau^k} e^{-\frac{\sinh 2r}{4}(t^2+\tau^2)+t\tau \cosh^2 r} \Big|_{t,\tau=0}, \end{aligned} \quad (32)$$

as well as

$$\begin{aligned} N_{k,k+2} &\equiv \langle b^{\dagger 2} \rangle_{\text{PASVS}} \\ &= \frac{\partial^{2k+2}}{\partial t^k \partial \tau^{k+2}} e^{-\frac{\sinh 2r}{4}(t^2+\tau^2)+t\tau \cosh^2 r} \Big|_{t,\tau=0} \end{aligned} \quad (33)$$

Then, according to Eqs. (9) and (31), we can directly obtain the Quantum Fisher information of the MZI as

$$F_{QA} = 2\bar{n}_z\bar{n}_a + \bar{n}_z + \bar{n}_a - 2\bar{n}_z \frac{N_{k+2,k}}{N_k}, \quad (34)$$

where we have also set  $\theta = 0$  (the phase of the coherent state) for obtaining the good phase uncertainty and used

the relation  $N_{k+2,k} = N_{k,k+2}$ . For  $k = 0, 1, 2$ , combining Eqs. (25-28) and Eq. (34), we can analytically prove that the quantum Cramér-Rao bound can be reached via the parity detection in the limit  $\varphi \rightarrow 0$ . For general  $k$ , we can numerically prove this is still true.

Using the similar method, we derive the quantum Fisher information for the PSSVS-coherent interferometer state

$$F_{QS} = 2\bar{n}_z\bar{n}_s + \bar{n}_z + \bar{n}_s - 2\bar{n}_z \frac{C_{l+2,l}}{C_l}, \quad (35)$$

where

$$\begin{aligned} C_{l+2,l} &\equiv \langle b^2 \rangle_{\text{PSSVS}} \\ &= \frac{\partial^{2k+2}}{\partial t^{k+2} \partial \tau^k} e^{-\frac{\sinh 2r}{4}(t^2+\tau^2)+t\tau \sinh^2 r} \Big|_{t,\tau=0}, \\ C_{l,l+2} &\equiv \langle b^{\dagger 2} \rangle_{\text{PSSVS}} \\ &= \frac{\partial^{2k+2}}{\partial t^k \partial \tau^{k+2}} e^{-\frac{\sinh 2r}{4}(t^2+\tau^2)+t\tau \sinh^2 r} \Big|_{t,\tau=0}, \end{aligned} \quad (36)$$

and we have used the relation  $C_{l+2,l} = C_{l,l+2}$ . Similarly, we can check that the quantum Cramér-Rao bound can be reached via the parity detection in the limit  $\varphi \rightarrow 0$  for the PSSVS-coherent considered as the interferometer state.

#### V. CONCLUSIONS

In summary, we have studied the quantum optimal interference by mixing a coherent state with a PASVS. Given a constraint on the total average number of photons and in the limit of  $\varphi \rightarrow 0$ , for a MZI with PASVS-coherent and PSSVS-coherent as well as SVS-coherent input states, almost the same phase uncertainties can be obtained. However, when the phase shift  $\varphi$  somewhat deviates from zero, the optimal state is neither the SVS nor the PSSVS, but the PASVS when these three states contain many photons. On the other hand, for fixed the initial squeezing  $r$ , it is better to perform photon addition rather than photon subtraction for improving the phase sensitivity of the MZI. This may be because that it is always better to perform addition rather than subtraction in order to increase the average photon number of the SVS for given the initial squeezing. Finally, we show that the quantum Cramér-Rao bound can be reached via the parity detection in the limit  $\varphi \rightarrow 0$ .

#### ACKNOWLEDGMENTS

This work is supported by the National Natural Science Foundation of China (No. 11690032, No. 11665013, and No. 11704051) and sponsored by Qing Lan Project of the Higher Educations of Jiangsu Province of China.



- 
- [1] V. Giovannetti, S. Lloyd, and L. Maccone, "Advances in quantum metrology," *Nat. Phot.* **5**, 222–229 (2011).
- [2] L. Pezzè, A. Smerzi, M.K. Oberthaler, R. Schmied, and P. Treutlein, "Quantum metrology with nonclassical states of atomic ensembles," arXiv: 1609.01609v3 (2018).
- [3] C.M. Caves, "Quantum-mechanical noise in an interferometer," *Phys. Rev. D* **23**, 1693–1708 (1981).
- [4] Z.Y. Ou, "Fundamental quantum limit in precision phase measurement," *Phys. Rev. A* **55**, 2598–2609 (1997).
- [5] J.J. Bollinger, W.M. Itano, D.J. Wineland, and D.J. Heinzen, "Optimal frequency measurements with maximally correlated states," *Phys. Rev. A* **54**, R4649–R4652 (1996).
- [6] J. Dunningham and T. Kim, "Using quantum interferometers to make measurements at the Heisenberg limit," *J. Mod. Opt.* **53**, 557–571 (2006).
- [7] G. Gilbert, M. Hamrick, and Y.S. Weinstein, "Use of maximally entangled N-photon states for practical quantum interferometry," *J. Opt. Soc. Am. B* **25**, 1336–1340 (2008).
- [8] B.L. Higgins, D.W. Berry, S.D. Bartlett, H.M. Wisman, and G.J. Pryde, "Entanglement-free Heisenberg-limited phase estimation," *Nat. Lett.* **450**, 393–396 (2007).
- [9] H. Lee, P. Kok, and J.P. Dowling, "A quantum Rosetta stone for interferometry," *J. Mod. Opt.* **49**, 2325–2338 (2010).
- [10] C.C. Gerry, A. Benmoussa, and R.A. Campos, "Nonlinear interferometer as a resource for maximally entangled photonic states: Application to interferometry," *Phys. Rev. A* **66**, 013804 (2002).
- [11] M.W. Mitchell, J.S. Lundeen, and A.M. Steinberg, "Super-resolving phase measurements with a multiphoton entangled state," *Nature* **429**, 161–164 (2004).
- [12] G.Y. Xiang, B.L. Higgins, D.W. Berry, H.M. Wiseman, and G.J. Pryde, "Entanglement-enhanced measurement of a completely unknown optical phase," *Nat. Phot.* **5**, 43–47 (2011).
- [13] R. Demkowicz-Dobrzanski, M. Jarzyna, and J. Kolodynski, "Quantum Limits in Optical Interferometry," *Prog. Opt.* **60**, 345–435 (2015).
- [14] Q.S. Tan, J.Q. Liao, X.G. Wang, and F. Nori, "Enhanced interferometry using squeezed thermal states and even or odd states," *Phys. Rev. A* **89**, 053822 (2014).
- [15] S.Y. Lee, C.W. Lee, J. Lee, and H. Nha, "Quantum phase estimation using path-symmetric entangled states," *Sci. Rep.* **6**, 30306 (2016).
- [16] M.J. Holland and K. Burnett, "Interferometric detection of optical phase shifts at the Heisenberg limit," *Phys. Rev. Lett.* **71**, 1355–1358 (1993).
- [17] Z.Y. Ou, "Complementarity and Fundamental Limit in Precision Phase Measurement," *Phys. Rev. Lett.* **77**, 2352–2355 (1996).
- [18] L. Pezzè and A. Smerzi, "Ultrasensitive Two-Mode Interferometry with Single-Mode Number Squeezing," *Phys. Rev. Lett.* **110**, 163604 (2013).
- [19] S. Wang, Y.T. Wang, L.J. Zhai, and L.J. Zhang, "Two-mode quantum interferometry with a single mode Fock state and parity detection," *J. Opt. Soc. Am. B*, **35**, 1046–1053 (2018).
- [20] L. Pezzè and A. Smerzi, "Mach-Zehnder Interferometry at the Heisenberg Limit with Coherent and Squeezed-Vacuum Light," *Phys. Rev. Lett.* **100**, 073601 (2008).
- [21] K.P. Seshadreesan, P.M. Anisimov, H. Lee and J.P. Dowling, "Parity detection achieves the Heisenberg limit in interferometry with coherent mixed with squeezed vacuum light," *New J. Phys.* **13**, 083026 (2011).
- [22] C.C. Gerry and J. Mimih, "The parity operator in quantum optical metrology," *Contemp. Phys.* **51**, 497–511 (2010).
- [23] M.D. Lang and C.M. Caves, "Optimal Quantum-Enhanced Interferometry Using a Laser Power Source," *Phys. Rev. Lett.* **111**, 173601 (2013).
- [24] R. Birrittella and C.C. Gerry, "Quantum optical interferometry via the mixing of coherent and photon-subtracted squeezed vacuum states of light," *J. Opt. Soc. Am. B* **31**, 586–593 (2014).
- [25] J. Wenger, R. Tualle-Brouri, and P. Grangier, "Non-Gaussian Statistics from Individual Pulses of Squeezed Light," *Phys. Rev. Lett.* **92**, 153601 (2004).
- [26] A. Ourjoumtsev, A. Dantan, R. Tualle-Brouri, and P. Grangier, "Increasing Entanglement between Gaussian States by Coherent Photon Subtraction," *Phys. Rev. Lett.* **98**, 030502 (2007).
- [27] G.S. Agarwal and K. Tara, "Nonclassical properties of states generated by the excitations on a coherent state," *Phys. Rev. A* **43**, 492–497 (1991).
- [28] A. Zavatta, S. Viciani, and M. Bellini, "Quantum-to-Classical Transition with Single-Photon-Added Coherent States of Light," *Science* **306**, 660–662 (2004).
- [29] C.W. Helstrom, *Quantum Detection and Estimation Theory* (Academic Press, New York, 1976).
- [30] M.O. Scully and M.S. Zubairy, *Quantum Optics* (Cambridge University Press, New York, 1997).
- [31] S. Wang, H.C. Yuan, and X.X. Xu, "Conditional generation of Fock states and Schrödinger-cat states via adding multiple photons to a squeezed vacuum state," *Eur. Phys. J. D* **67**, 102 (2013).
- [32] X.G. Meng, Z. Wang, H.Y. Fan, and J.S. Wang, "Nonclassicality and decoherence of photon-subtracted squeezed vacuum states," *J. Opt. Soc. Am. B* **29**, 3141–3149 (2012).
- [33] M.S. Kim, "Recent developments in photon-level operations on travelling light fields," *J. Phys. B*, **41**, 133001 (2008).
- [34] M.B. Stephen, F. Gergely, R.G. Claire, and C.S. Fiona, "Statistics of photon-subtracted and photon-added states," *Phys. Rev. A*, **98**, 013809 (2018).
- [35] See, for example C. C. Gerry and P. L. Knight, *Introductory Quantum Optics* (Cambridge University Press, New York, 2005), Chap. 7.
- [36] B. Yurke, S.L. McCall, and J.R. Klauder, "SU(2) and SU(1,1) interferometers," *Phys. Rev. A* **33**, 4033–4054 (1986).
- [37] L. Cohen, D. Istrati, L. Dovrat, and H.S. Eisenber, "Super-resolved phase measurements at the shot noise limit by parity measurement," *Opt. Express* **22**, 11945–11953 (2014).
- [38] Y. Ben-Aryeh, "Phase estimation by photon counting measurements in the output of a linear Mach-Zehnder interferometer," *J. Opt. Soc. Am. B* **29**, 2754–2764 (2012).

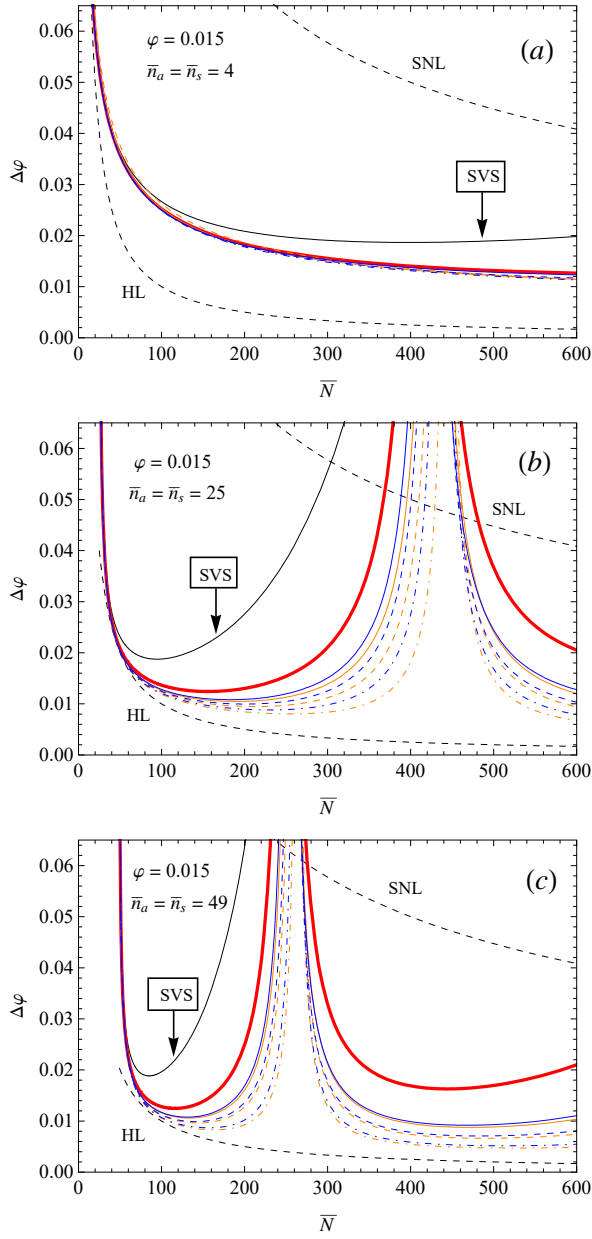


FIG. 6. Plots of the phase uncertainty versus the total average photon at  $\varphi = 0.015$  for fixed the average photon number of the PASVS and the PSSVS, as well as the SVS, along with the corresponding curves for the SNL and the HL limits. The thick red line represents the PASVS(or PSSVS)-coherent state with  $k = l = 1$ ; the orange line represents the PASVS-coherent state with  $k = 2$ ; the orange dashed line denotes the PASVS-coherent state with  $k = 3$ ; the orange dotted-dashed line denotes  $k = 6$ . While, the blue line represents the PSSVS-coherent state with  $l = 2$ ; the blue dashed line represents  $l = 3$ ; the blue dotted-dashed line denotes  $l = 6$ .

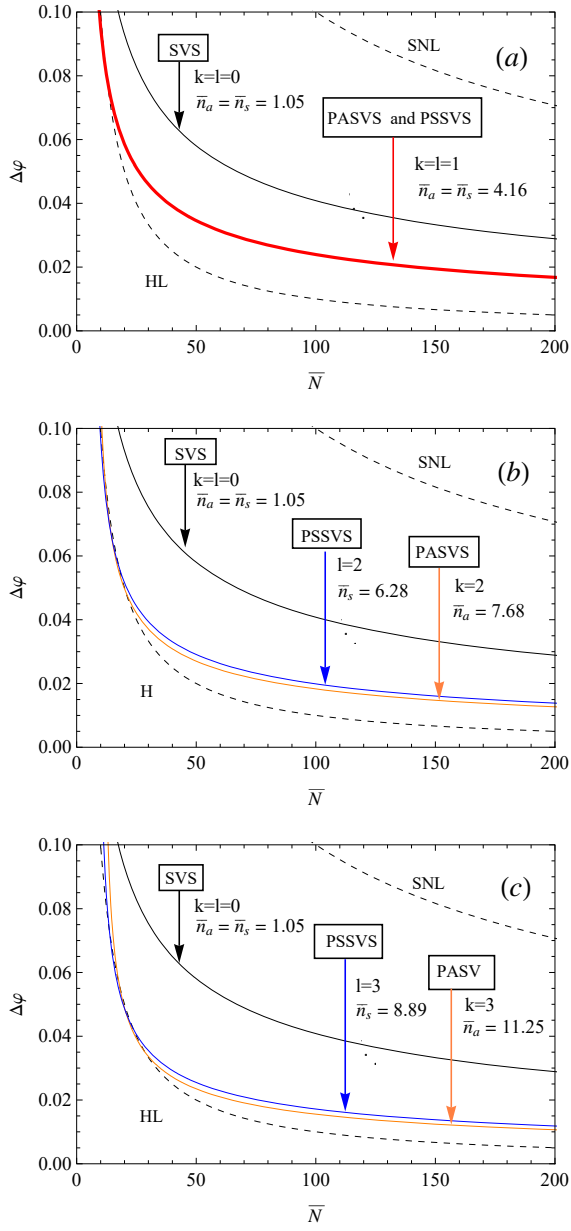


FIG. 7. For  $r = 0.9$ , plots of the phase uncertainty versus the total average photon number at  $\varphi = 10^{-4}$ , along with the corresponding curves for the SNL and HL limits. Only the parameter  $l$  is being changed.